X-ray Absorption Spectroscopy Analysis of Heavy Metals by Means of a Silicon Detector

S. M. Osadchii[a], *, A. A. Petukhov[a], and V. B. Dunin[b]

[a]*All-Russian Research Institute of Physical-Technical and Radiotechnical Measurements, Mendeleevo, Moscow oblast, 141570 Russia*
[b]*Joint Institute for Nuclear Research, Dubna, Moscow oblast, 141980 Russia*
*e-mail: osm@vniiftri.ru

Abstract—A Si-PIN detector with longitudinal arrangement of the silicon wafer for detecting X-ray quanta with an energy of up to 100 keV is designed. Its resolution is estimated. An X-ray absorption spectroscopy method for the detection of heavy metals at the K-absorption edges is implemented using the designed detector. The results of measuring the thicknesses of lead and gold foils placed behind a shield by the X-ray absorption spectroscopy method and with a micrometer gauge are compared. The detection limits of heavy metals behind steel or aluminum shields are determined. The measurement error of the metal-foil thicknesses is estimated.

INTRODUCTION

In most practical applications, for example, in the case of baggage check, the enrichment of ores, and sorting of scrap or waste electronic equipment, there is a need to detect certain chemical elements. Despite the abundance of instruments and methods for elemental analysis, there are very few real devices that can be built into existing conveyor processing systems and possess the necessary performance to detect certain chemical elements in objects on a conveyer. With the aid of magnets, only alloys containing iron can be detected. X-ray scanners make it possible to determine three groups of elements [1–3], and all elements with an atomic number of $Z = 18$ and higher belong to one group. Typical scanners cannot detect some heavy elements, such as gold, lead, mercury, and thallium. It is difficult to increase the resolution of scanners because they are based on photodiode and scintillation detectors with a low energy resolution. The greatest achievement for scanners is the possibility to distinguish four groups of elements and one group of three light elements in the scanning process.

The most common method for analyzing the elemental composition is X-ray fluorescence analysis (XRF) [4–6]. It is based on the dependence of the intensity of X-ray fluorescence at lines of the K and L series on the concentration of the chemical element in the sample. X-ray radiometric methods determine the content of extracted rocks in ore for further sorting [7].

The characteristic fluorescence radiation of atoms, the intensity of which is proportional to the concentration of these atoms in the sample, appears when the sample is irradiated with a powerful flux of quanta from an X-ray tube. As a rule, fluorescence radiation is recorded by an energy dispersive detector. The overwhelming majority of XRF energy dispersive detectors are silicon drift SDD or PIN detectors doped with lithium [5, 8]. The production technology of such detectors is well developed. The typical thickness of the sensitive layer of silicon PIN and SDD detectors is 0.3–0.5 mm. Heavy metals are recorded by X-ray fluorescence analysis using such detectors only at lines of the L series (less than 15 keV), while the detection efficiency of lines of the K series is low and silicon detectors in this energy range are basically not used. Limiting the operating range to about 15 keV means that if the detected heavy element is surrounded by another material, even with a lower atomic number, then the fluorescence radiation at lines of the L series will be strongly absorbed in the shielding material. Let us estimate, using the reference data [9, 10], the X-ray losses in a 6-mm-thick steel sample: near the absorption edges of Au at 80.725 keV and Pb at 88.00 keV, the loss is about 60%; near the characteristic lines of Au (9.71–13.38 keV) and Pb (10.55–14.76 keV) in the L series, the losses reach 99.9997%.

These estimates show that if a sample of gold or lead is shielded by a steel screen, the XRF method is

not applicable. There are also restrictions on the geometrical arrangement of detectors. An XRF detector is difficult to use in a scanner, since the detector would have to be at a distance of more than 80 cm to examine the material in a scanner with a 60 × 80 cm window, which would lead to a significant loss in sensitivity and a strong effect of scattering from the inside surface of the scanner tunnel. Due to the above difficulties, XRF and X-ray scanners with existing detectors cannot solve the problem of determining the atomic number of a heavy metal surrounded by a layer of material.

To date, an X-ray absorption spectroscopy analysis (XASA) technique has been developed, which applies attenuation of the flux of X-ray or gamma-ray quanta. Their energy values are on opposite sides of the absorption edge of the element being analyzed [11–14]. In this work, the possibility of using the XASA method for the express determination of heavy metals in conveyor systems is considered and the resolution of the method is estimated. The method of spectral analysis is effectively used for monitoring the contents of lead in gasoline, chlorine in organic compounds, and uranium in solutions of its salts. Previously, in cases of monitoring the content of lead in gasoline, the absorbance in the ultraviolet region of the spectrum was measured. In [13], the possibility of using X-ray absorptiometry to determine the density of aqueous salt and aqueous alcohol solutions is shown. In [14], XASA was used to control the parameters and structure of the liquid and gas flows in a pipeline by means of a ^{241}Am radiation source and a NaI(Tl) scintillation detector.

To determine heavy metals by the XASA method, a device with a detector possessing the necessary response rate when the analyzed material moves along a conveyor, operating at room temperature without additional cooling, and having sufficient resolution and an upper limit of the operating range of about 100 keV is required. For these purposes, gamma-ray spectrometry uses detectors based on CdTl (CdZnTl) [9]. Due to the fact that silicon detectors are widely used in X-ray scanners and the technology of their manufacture is well-established, this study considers the possibility of using Si-PIN detectors for the XASA of heavy metals at lines of the K series in a special configuration when X-ray radiation is directed along a layer, i.e., along the long side of the detector. The detector used in the measurements was developed for X-ray diffraction analysis [15] and then modified for use in XASA in the framework of this study. The detector dimensions are as follows: the width is 1.5 mm, the length is 12 mm, and the silicon-wafer thickness is 0.5 mm. A bias voltage of 80 V was applied to the plate electrodes. The total conversion coefficient of the charge-sensitive amplifier is 1 mV per 100 electrons. According to calculations carried out on the basis of the data given in [16], the recording efficiency of quanta with an energy of 80 keV in this geometry increases from 5 to 70% in comparison with the case of a silicon detector

plate arranged perpendicular to the direction of propagation of X-ray quanta. The spatial resolution with such geometry, i.e., when X-ray radiation is directed along a layer, is quite acceptable for scanners and can be about 0.5–1.5 mm. The lack of forced cooling eliminates problems with evacuating the detector and substantially simplifies its design.

In this study, the efficiency of the XASA method using the developed detector is theoretically analyzed and experimentally evaluated. In the considered cases, a small amount of a heavy-metal element is located behind a screen made of a metal with a lower atomic number. For example, a microcircuit with gold-plated contacts is mounted in a device case with steel walls or a device electronic board made with the use of copper contacts coated with lead solder is mounted into an aluminum case. For these cases, the detection limits are experimentally determined and the error in measuring the thickness of the gold coating and the lead layer is estimated.

EXPERIMENTAL

The experimental setup is shown in Fig. 1. In the proposed geometry, the silicon detector is oriented with the end face toward the received radiation; the area of the end of the Si-PIN detector is 0.75 mm^2. A RAPAN X-ray radiation source and an X-ray tube with a tungsten anode were used in the setup. The voltage in the tube was $U = 150$ kV and the current was $i = 0.16–1$ mA. To measure the spectra, a V4K-SATsP-USB analyzer was used [17]. The detector was located at a distance of 820 mm from the X-ray tube, so that an extended object could be placed in the illuminated volume, as in a typical X-ray scanner window with a size of 60 × 80 cm. The X-ray source, the detector, and the metal under study were placed in a SAT-URN X-ray transmission integrated unit [2], the lead shield of which protected against scattered radiation. The intensity of the tube radiation is very high at K lines of tungsten and at lower values of energy, which causes a large load of the detector. To eliminate this problem, a filter made of materials with small atomic numbers was used to correct the spectrum and ensure normal operation of the detector, which was located behind the collimator of the tube. The detector was placed in a lead case with a wall thickness of 2 mm. The thickness of the lead collimator of the detector was 10 mm, and the aperture diameter in the collimator was 3.5 mm.

The absorption spectra of lead films of different thickness are shown in Fig. 2. The vertical lines show the energy windows, in which the intensity on either side of the absorption edge was calculated by integration. The interval between the energy windows was close to the energy resolution of the detector. A ^{241}Am source was used to calibrate the energy scale. For com-
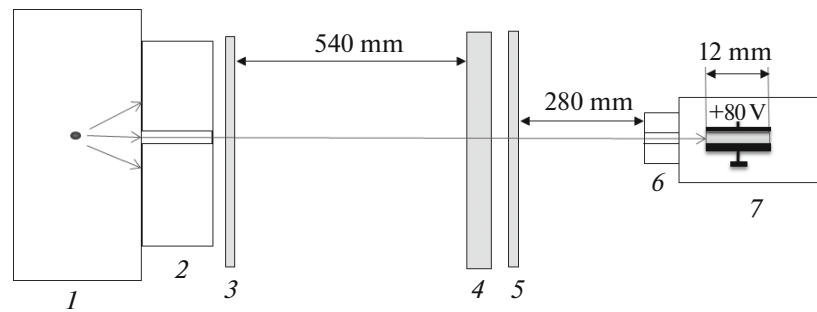
Fig. 1. Scheme of the experiment: *1* is an X-ray tube; *2* is a lead collimator; *3* is a low energy filter; *4* is a screen; *5* is a sample; *6* is a lead collimator of the detector; *7* is a detector in a lead case.

parison, this figure shows the position of the absorption edge of gold.

Detailed interpretation of the spectra is complicated by Compton scattering, which is large in silicon at these energy values [16]. Two peaks corresponding to the characteristic lines of tungsten, of which the anode is made, are seen in the graphs and a decrease in the intensity of bremsstrahlung radiation to an energy of 150 keV corresponding to a maximum voltage of 150 V in the X-ray tube is observed.

RESOLUTION OF THE SILICON DETECTOR

Estimation of the detector resolution gives an energy resolution of 1.4 keV on the MoK_α line at 17.4 keV in the operation mode without forced cooling at an ambient temperature of 22°C (8% when converted to the relative resolution) and an energy resolution of 1.65 keV on the ^{241}Am source line at 59.5 keV (2.8% when converted to the relative resolution), which are comparable to the energy resolution of detectors based on CdZnTe [5, 17]. The comparable energy resolution on the line at 59.5 keV is explained by the influence of two different factors: a larger number of charge carriers are formed from a single quantum in silicon and a smaller number of quanta interact with the formation of carriers because of the Compton effect.

An estimate of the detector resolution from the broadening of the absorption jump in the absorption spectra of lead (Fig. 2) gives a relative resolution of 1.8 keV near the absorption edge at 88 keV. To study the detector resolution, the fluorescence spectrum of lead in the range from 50 to 100 keV was also measured (Fig. 3). The resolution on the line at 84.94 keV was 2.36 keV, which coincides with the previous measurements. If we compare estimates of the detector resolution for different energy values, then the absolute resolution increases with an increase in energy, while the relative resolution decreases. This is consistent with formula (1) [18−20] for estimating the energy resolution of the detector ΔE:

$$\Delta E = \sqrt{\Delta E_d + \Delta E_n}, \qquad (1)$$

where $\Delta E_d = 2.36\sqrt{FEw}$ is the energy resolution of the detector, which is determined by the fluctuation of the number of pairs of created carriers (theoretical limit); and $\Delta E_n \approx 2\left(\dfrac{w}{e}\right)\sqrt{kTC}$ is the noise of the charge sensitive amplifier.

From Eq. (1) at the Fano factor $F = 0.1$, the energy of formation of an electron−hole pair is $w = 0.0035$ keV for silicon, the capacitance is $C \approx 0.4$ pF, the temperature is $T = 295$ K, and the elementary charge is e; the ΔE resolution values (Table 1) are obtained for energy values corresponding to the characteristic lines of a ^{57}Co source at 6.4 and 14.4 keV and of a MoK_α source at 17.4 keV and to the energy of the absorption edge of lead at 88 keV (Fig. 3).

The difference between the measured resolution and the numerical estimate from Eq. (1) is explained by incomplete charge collection, measurement errors, inaccurate estimation of the capacitance C and other
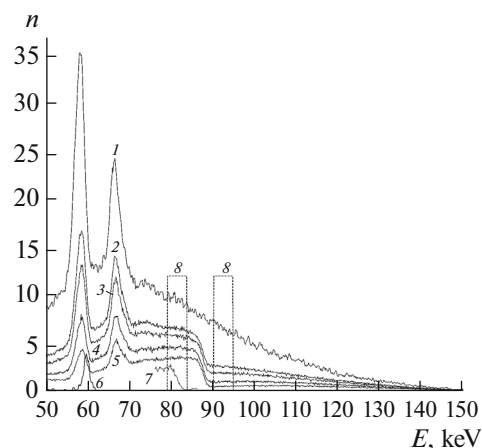
Fig. 2. (*1*) X-ray spectrum without a sample; X-ray absorption spectra of lead foils with thicknesses of (*2*) 0.15, (*3*) 0.2, (*4*) 0.3, and (*5*) 0.4 mm; (*6*) the X-ray spectrum of ^{241}Am ($E = 59.5$ keV); (*7*) X-ray absorption spectrum of a gold foil; (*8*) energy windows; n is the number of counts in the spectrometer channel.
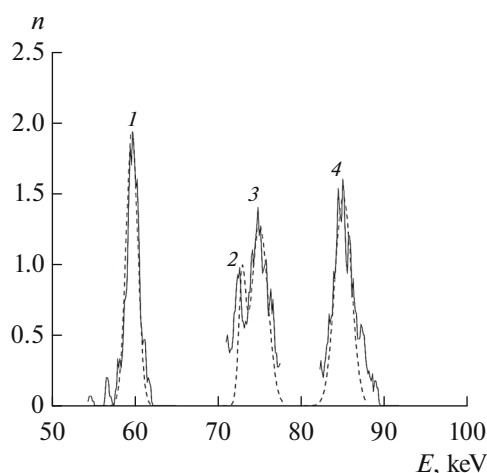
Fig. 3. Spectra of (*1*) the ^{241}Am source ($E = 59.5$ keV) and fluorescence radiation of (*2*) Pb$K_{\alpha 2}$ ($E = 72.8$ keV), (*3*) Pb$K_{\alpha 1}$ ($E = 74.97$ keV), and (*4*) PbK_β ($E = 84.94$ keV) sources. The dashed lines show the approximation of the spectra by the Gaussian function; *n* is the number of counts in the spectrometer channel.

factors. Comparison of these results with the results obtained in [21] shows a good agreement given the results of comparison of the geometric dimensions of the detectors and the ratios of the measured energy resolutions.

The temperature dependence of the energy resolution with small temperature changes, for example, with a deviation of 5°C from a temperature of 22°C, at which the measurements were carried out, is about 0.8%. If temperature deviations are more significant (for example, a device that implements XASA is used in a wide temperature range), a temperature correction should be introduced for instrument calibration.

ANALYSIS OF THE POSSIBILITY OF DETERMINING THE SAMPLE THICKNESS FROM THE ABSORBANCE JUMP

The relationship between the incident radiation intensity I_0, transmitted radiation intensity I, and

Table 1. Energy resolution of the silicon detector

E, keV	Calculation		Experiment	
	ΔE, keV	$\Delta E/E$, %	ΔE, keV	$\Delta E/E$, %
6.4	1.71	26.3	1.65	25.4
14.4	1.72	11.9	1.67	11.6
17.4	1.72	9.9	1.4	8.0
59.5	1.77	3.0	1.65	2.8
74.75	1.78	2.4	2.36	3.2
84.9	1.79	2.1	2.36	2.8
88	1.80	2.0	1.80	2.0

coordinate x along the beam-propagation direction is determined by the following formula:

$$\mu_{h,l} x = -\ln\left(\frac{I}{I_0}\right)_{h,l}, \qquad (2)$$

where μ is the linear absorption coefficient, and the h and l indices refer to the energy windows above and below the absorption edge, respectively. The relative intensity (Fig. 1) is the number of counts, n, per time interval corresponding to energy E in the spectrometer channel. The x coordinate in Eq. (2) is measured in length units, and μ is measured in inverse length units. According to [10], μx can be expressed as $x\rho(\mu/\rho_t)$, where ρ_t is the reference value of the density and ρ is the density of the used material. A detailed expression for the relationship, which takes into account the explicit dependence on the energy near the absorption edge, is given in [22]; in this study, we used the generalized form of Eq. (2).

The spectral distribution of the intensity of bremsstrahlung X-ray radiation, i.e., the emission spectrum of the X-ray tube without considering its attenuation in the target and outlet window, can be determined using Kramers' formula:

$$I_0(E) = k_0 Z i (eU/E - 1), \qquad (3)$$

where Z is the atomic number of the anode material of the X-ray tube; k_0 is the proportionality coefficient, the dimension of which depends on the measurement method: if I_0 is measured by the number of counts per second [s^{-1}], then the dimension of k_0 is [s^{-1} A^{-1}]. The spectrum (Fig. 2) in the region above the characteristic lines of the X-ray-tube anode differs from the spectrum described by Eq. (3). This is due to the fact that the sensitivity of the detector depends on the energy of X-ray quanta. The dependence of the detector sensitivity on the energy in a small interval near the absorption edge can be taken into account by replacing k_0 with the following expression:

$$k_0[1 - k_1(E/E_s)], \qquad (4)$$

where E_s is the energy of the absorption edge, and k_1 is the dimensionless coefficient of proportionality. Using Eqs. (2)–(4), the following expression can be obtained for the energies below (I_l) and above (I_h) the absorption edge:

$$x_a[\mu_l(E_l) - \mu_h(E_h)] = [\ln(I_h/I_{0h}) - \ln(I_l/I_{0l})]. \quad (5)$$

In the limit of narrow windows near the absorption edge, the following formula is obtained from Eq. (5):

$$x_a = \frac{\ln(I_h/I_l)}{\mu_l(s-1)}, \qquad (6)$$

where s is the absorbance jump. The energy window is considered narrow if the change in the source energy and receiver sensitivity is small within the window.

In the case of wide windows, the following formula is obtained near the absorption edge by integrating Eq. (5) over energy in the interval of selected energy windows:

$$x_a = -\left(\int\limits_{E_{hm}-E_b}^{E_{hm}+E_b} \ln\left(\frac{I_h}{I_{0h}}\right)dE - \int\limits_{E_{lm}-E_b}^{E_{lm}+E_b} \ln\left(\frac{I_l}{I_{0l}}\right)dE\right) \Bigg/ \left(\int\limits_{E_{hm}-E_b}^{E_{hm}+E_b} \mu_h(E_h)dE - \int\limits_{E_{lm}-E_b}^{E_{lm}+E_b} \mu_l(E_l)dE\right), \qquad (7)$$

where x_a the metal-film thickness measured by the XASA method; E_{lm} and E_{hm} are the mean values of the energy of the windows; and E_b is the half width of the windows. The fine structure of the absorption edges was not taken into account in Eq. (7).

For narrow windows (6), a linear dependence of the x_a value on the thickness, l_m, measured by a micrometer gauge is assumed. The following factors affect the linearity and x_a measurement error: the fine structure of the absorption edges, the noise of the detector, and the fluorescence radiation of the collimators. In the case of wide windows (7), the dependence of the sensitivity coefficient of the detector on the energy (4) and the nonuniformity of the emission spectrum of the X-ray tube (3) are manifested in addition to the above factors affecting the linearity and measurement error. Expression (7) is too cumbersome to calculate for all detector cells at the operating speed of the conveyor, so it was simplified to reduce the calculation time. It should be noted that it is more convenient and faster to calculate $\ln\left(\int I_h dE \Big/ \int I_{0h} dE\right)$ instead of $\int \ln\left(I_h / I_{0h}\right)dE$ from the point of view of hardware resources and computational functions. In this case, there are no strict requirements imposed on the spectrum analyzer and the detector resolution. The pulses from all channels within a wide window are summed and then the logarithm of the ratio is calculated. If the voltage in the tube and its current are stable, then can be used formula I_{0l}, $I_{0h} = I_0(E_{l,h})$; which takes into account the dependence k_0 on energy formula (4); the $I_0(E_{l,h})$ values are determined by Eqs. (3). Integration in the denominator gives a value that depends only on the atomic number and the width of the window. A set of such values may be stored in the calculating device.

MEASURING THE THICKNESS OF METAL FILMS BY THE XASA METHOD

The effectiveness of the proposed method for analyzing heavy metals was experimentally verified using a setup whose diagram is shown in Fig. 1. Experiments were conducted, in which the element to be analyzed was lead and the material behind which it is located was a 6-mm-thick steel sheet in one case, and 16-mm-thick aluminum and 1.2-mm-thick copper sheets in the other case. Figure 4 illustrates the comparison of

the lead-foil thicknesses measured by the XASA method (l_a) and with a micrometer gauge (l_m).

Since the sample under study consisted of several layers of technical foil, the exact calculation of the absolute thicknesses by Eq. (7) is impeded by a lack of accurate values of the density, the elemental composition of the material, and the spectral sensitivity of the detector. Therefore, calibration by means of a reference sample with the maximum thickness was performed after measurements. The B type uncertainty [23] was assumed to be zero for this thickness.

The l_a value linearly depends on the l_m value in the range from 0.02 to 0.4 mm. When the sample thickness is more than 2 mm, the dependence becomes nonlinear. This is due to the fact that the intensity I decreases and the noise level of the detector begins to have an effect. Above all, linearity is important for the processing algorithm and the rapid quantitative determination of the chemical-element content. The detection limits of an element depend on the measurement error. If calibration and measurements were carried out with the same steel screen, the measurement error
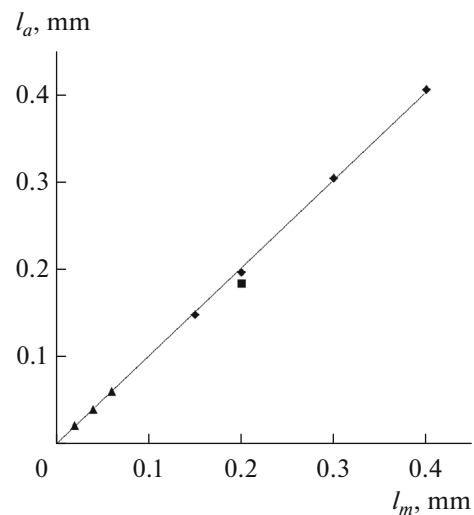
Fig. 4. Alignment of the lead-foil thicknesses measured by the XASA method (l_a) and with a micrometer gauge (l_m): rhombs correspond to the first series of measurements with a 6-mm-thick steel screen; triangles correspond to the second series of a 6-mm-thick steel screen; squares correspond to the measurements of a 0.2-mm-thick lead foil behind a two-layer screen comprised of 1.2-mm-thick copper and 16-mm-thick aluminum sheets; $l_a = x_a k$, where k is the calibration coefficient determined from the equality $l_a = l_m$ at $l_m = 0.4$ mm.
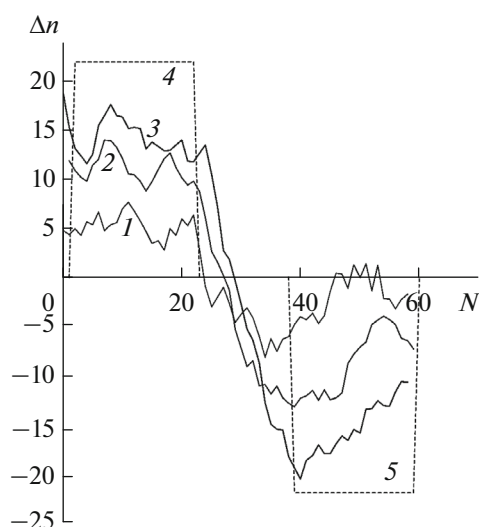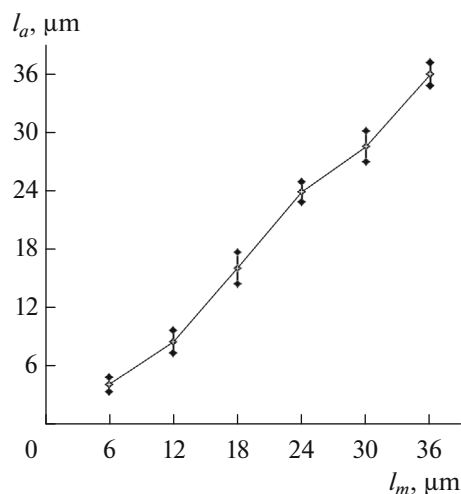
Fig. 5. Absorption spectra near the absorption edge (E = 80.725 keV) of gold foils with thicknesses of (*1*) 12, (*2*) 24, and (*3*) 36 μm. The energy windows selected (*4*) below the absorption edge and (*5*) above the absorption edge; N is the spectrometer-channel number; Δn is the number of counts in the channel minus the average number of counts over all channels.

Fig. 6. Alignment of the gold-foil thicknesses measured by the XASA method (l_a) and with a micrometer gauge (l_m). The vertical lines show the A type uncertainty in ten measurements; $l_a = x_a k$, where k is the calibration coefficient determined from the equality $l_a = l_m$ at $l_m = 36$ μm.

is about 5 μm. If screens made of different materials are used (a steel screen for calibration, and copper and aluminum screens for measurements), then the assessment gives a resolution of 18 μm in the case of measuring the lead-foil thickness. Replacing the screen material (steel, copper, and aluminum) affects both the change in the intensity of the X-ray quanta flux from the X-ray tube and the change in the spectrum given by Eq. (7). Both factors lead to an increase in the measurement error.

In the spectrum of a gold sample, the absorption edge corresponds to 80.725 keV (Figs. 2 and 5). Figure 5 shows the deviations of the intensity from the average value near the absorption edge for various gold-foil thicknesses. As is seen from Fig. 5, the energy corresponding to the measured absorbance jump slightly increases with an increase in the thickness, but this change is small and does not affect the thickness measurements. Experiments on measurements of the thickness by the XASA method were carried out, in which gold foil samples with thicknesses of 6 to 36 μm

Table 2. Uncertainty in measuring the gold-foil thickness by the XASA method

Thickness, μm	6	12	18	24	30	36
Uncertainty of type A, μm	1.5	2.3	3.2	2.1	3.1	2.4
Uncertainty of type B, μm	1.1	2.0	1.1	0.1	0.8	0
Total standard uncertainty, μm	1.9	3.1	3.4	2.1	3.2	2.4

were placed behind a steel screen with a thickness of 6 mm. For comparison, the gold-foil thicknesses measured by the XASA method and with a micrometer gauge are shown in Fig. 6. In contrast to the previous experiment, the spectrum was measured 10 times, and ten thickness values and then their mean, as well as the A and B type uncertainties, were calculated [23]. The measurement uncertainties calculated for each series is given in Table 2. In further calculations, an expanded uncertainty averaged over six series was used, which is 2.7 μm. Energy windows with a width of about 3.5 keV were chosen, and the interval between them was about 3 keV. With such energy windows for calculating the foil thickness, x_a, formula (6) for narrow windows is valid.

Figure 4 demonstrates that the dependence of the l_a value on the l_m value is close to a linear dependence in the range from 0.006 to 0.036 mm under the selected experimental conditions. With a distance of 820 mm between the X-ray tube and the detector, the relative standard uncertainty of the weight measurement, i.e., the ratio of the minimum weight of the sample per unit area to the weight of the shield per unit area, is 0.1%; the minimum weight of the detected metal gold is 0.15 mg. Similar estimates for the heavy metal thallium show that such indicators are sufficient to detect microdoses from 0.1 mg of thallium in a steel cell with a wall thickness of up to 3 mm. To simplify the spectrum-analyzer scheme and reduce the acquisition time, a two-channel analyzer with fixed windows can be implemented using the example of the detector described in [15]. By changing the threshold levels of the detector, one can retune the analyzer for the required metal. By expanding the windows to the level

of currently used scintillators, it is possible to obtain a distribution over atomic number groups and an object image that are standard for scanners.

The processing algorithm in the approximation of Eq. (6) boils down to calculation of the logarithm of the intensity ratio, which can be done quite rapidly. However, the total measurement time may be longer, which will slow down the speed of the conveyor in the scanner. Additional ways to reduce the measurement time are as follows: an increase in the current of the X-ray tube, transition to a pulsed mode of synchronous detection, and a decrease in the distance between the X-ray tube and the detector.

The method can be applied in sorters, X-ray scanners, and inspection machines [4] when needed to isolate heavy metals. The protocol, in which all items are first analyzed in the standard mode and then selected objects with large atomic numbers that are darkened in the picture are analyzed additionally on scanners with the option to control certain elements, is an operating option for scanners.

The proposed approach can be applied to determine the content of precious metals in the ore of extracted rocks and for further sorting. To extend the functionality in one scanner, two detectors tuned to different metals can be used.

CONCLUSIONS

The design of a Si-PIN detector with longitudinal arrangement of a silicon wafer for detecting quanta with energies of up to 100 keV is proposed and implemented. It is shown that the detection efficiency in such a geometry is significantly higher compared to the geometry of a detector silicon plate arranged perpendicular to the direction of propagation of X-ray quanta. The detection efficiency is sufficient to implement the X-ray absorption spectroscopy analysis method at the absorption edges of the *K* series of heavy metals.

The detector resolution is estimated; good agreement between the numerical estimates and measured values is demonstrated. It is shown that the relative energy resolution in the range of 60−90 keV is 2.0−3.2% at a temperature of 22°C and meets the level of widely used detectors based on CdTl (CdZnTl) and Ge.

The thicknesses of lead and gold foils measured by the XASA method behind a screen and with a micrometer gauge are compared and analyzed. The detection limits are determined, and the errors in measuring the thicknesses of lead and gold foils are estimated. It is shown that the XASA method can be used for creating industrial scanners capable of detecting heavy metals behind a screen, for example, in the process of the enrichment of ores with heavy metals, determining precious metals in waste electronic products, or detecting unauthorized items during luggage inspection.

REFERENCES

1. R. Ch. Bokun, and S. M. Osadchii, J. Surf. Invest.: X-Ray, Synchrotron Neutron Tech. **4** (4), 591 (2010).

2. S. M. Osadchii, *Abstracts VII Natl. Conf. "X-Ray, Synchrotron Radiation, Neutrons and Electrons for Nanosystems and Materials Research. Nano-Bio-Info-Cognitive Technologies"* (Moscow, 2009), p. 506 [In Russian].

3. www.smithsdetection.com/products(SmithDetection)

4. R. Jenkins, in *Encyclopedia of Analytical Chemistry*, Ed. by R. A. Meyers, (John Wiley & Sons Ltd., Chichester, 2000), p. 13269.

5. www.bruker.com/products/x-ray-diffraction-and-elemental-analysis/x-ray-fluorescence.html (Bruker Corporation)

6. J. Kawai, in *X-Ray Spectrometry: Recent Technological Advances*, Ed. by K. Tsuji, (Wiley, Chichester, 2004), p. 405.

7. *The X-Ray Radiometric Methods in Search for, and Prospection of, Ore Deposits,* Ed. by A. P. Ochkur (Nedra, Leningrad, 1985) [in Russian].

8. http://amptek.com/si-pin-vs-cdte-comparison (Amptek)

9. https://physics.nist.gov/PhysRefData/XrayMassCoef/tab3.html (NIST)

10. *X-Ray Technology. A Reference Book,* Ed. by V. V. Klyuev (Mashinostroenie, Moscow, 1992) [in Russian].

11. D. F. Sanchez, A. S. Simionovici, L. Lemelle, et al., Sci. Rep **7,** 1 (2017).

12. J. L. Glover and C. T. Chantler, Meas. Sci. Tech., No. 18, 2916 (2007).

13. N. A. Antropov, D. A. Karpov, Yu. Yu. Kryuchkov, and T. N. Strezhneva, Izv. Tomsk. Politekh. Univ. **318** (2), 136 (2011).

14. R. Hanus, M. Zych, M. Kusy, et al., Flow Meas. Instrum, No. **60**, 17 (2018).

15. S. M. Osadchii, P. P. Kovalenko, and I. G. Tolpekin, *Abstracts VI Natl. Conf. on the Use of X-Ray, Synchrotron Radiation, Neutrons and Electrons for Materials Research* (Moscow, 2009), p. 618 [In Russian].

16. G. V. Fetisov, *Synchrotron Radiation. Methods for Structural Analysis of Matter* (Fizmatlit, Moscow, 2007).

17. www.parsek.ru

18. S. Sordo, L. Abbene, E. Caroli, et al., Sensors **9,** 3491 (2009).

19. N. B. Strokan, A. M. Ivanov, A. A. Lebedev, et al., Semiconductors **39** (12), 1420 (2005).

20. S. F. Baldin, N. A. Vartanov, Yu. V. Erykhailov, et al., *Applied Spectrometry with Semiconductor Detectors* (Atomizdat, Moscow, 1974) [in Russian].

21. G. P. Vasiliev, V. K. Voloshyn, O. S. Deiev, et al., J. Surf. Invest.: X-Ray, Synchrotron Neutron Tech. **8** (2), 391 (2014).

22. A. G. Tur'yanskii, S. S. Gizha, V. M. Senkov, and S. K. Savel'ev, Tech. Phys. Lett. **40** (4), 346 (2014).

23. *GOST (State Standard) R 54500.3*-2011 */ ISO/IEC Guide 98-3:2008.* Uncertainty of Measurement. Pt. 3.

Translated by O. Kadkin